J Neurophysiol 108: 2931–2945, 2012.
First published September 12, 2012; doi:10.1152/jn.00512.2011.

An evaluation of in vivo voltage-sensitive dyes: pharmacological side effects and signal-to-noise ratios after effective removal of brain-pulsation artifacts

T. H. Grandy,[1,2] S. A. Greenfield,[1] and I. M. Devonshire[1]

[1]*Department of Pharmacology, University of Oxford, Oxford, United Kingdom; and* [2]*Institute of Neurophysiology, Charité Universitätsmedizin Berlin, Berlin, Germany*

Submitted 13 June 2011; accepted in final form 11 September 2012

Grandy TH, Greenfield SA, Devonshire IM. An evaluation of in vivo voltage-sensitive dyes: pharmacological side effects and signal-to-noise ratios after effective removal of brain-pulsation artifacts. *J Neurophysiol* 108: 2931–2945, 2012. First published September 12, 2012; doi:10.1152/jn.00512.2011.—In the current study, we investigated pharmacological side effects and signal-to-noise ratios (SNRs) of two commonly used voltage-sensitive dyes (VSDs): the blue dye RH-1691 (1 mg/ml) and the red dye di-4-ANEPPS (0.1 mg/ml), applied in vivo to the rat barrel cortex. Blue dyes are often favored over red dyes in in vivo studies due to their apparent superior SNR, partly because their fluorescence spectrum is farther away from the hemoglobin absorption spectrum, making them less prone to heartbeat-associated brain-pulsation artifacts (BPA). We implemented a previously reported template-based BPA removal algorithm and evaluated its applicability to di-4-ANEPPS before comparing characteristics of the two dyes. Somatosensory-evoked potentials (SEPs) were also recorded. Whereas SEPs recorded before and after application of di-4-ANEPPS failed to exhibit demonstrable differences, RH-1691 caused a significant and prolonged increase in SEP amplitude for several hours. In contrast, neither dye influenced the spontaneous cortical activity as assessed by the spectral content of the EEG. Both dyes turned out to be strikingly similar with respect to changes in fractional fluorescence as a function of SEP response amplitude, as well as regarding shot noise characteristics after removal of the BPA. Thus there is strong evidence that the increased SNR for RH-1691 is a consequence of an artificially increased signal. When applying an appropriate BPA removal algorithm, di-4-ANEPPS has proven to be suitable for single-trial in vivo VSD imaging (VSDI) and produces no detectable neurophysiological changes in the system under investigation. Taken together, our data argue for a careful re-evaluation of pharmacological side effects of RH-1691 and support the applicability of di-4-ANEPPS for stable single-trial in vivo VSDI recordings.

rat; barrel cortex; anesthesia; toxicity; di-4-ANEPPS; RH-1691

WHEREAS IMAGING METHODOLOGIES have proven highly popular with neuroscientists, the advantages and disadvantages of each particular technique must be carefully considered before selecting the most appropriate (Grinvald and Hildesheim 2004). For instance, the spatial resolution of imaging techniques has improved gradually over the years, and we can now visualize biochemical changes within different compartments of an individual cell in real time. Techniques that examine processes at such high spatial resolution, however, often require the use of dyes to enable the process being studied to be visualized with high contrast. In such cases, in addition to the necessary estimation of the signal-to-noise ratio (SNR) of the respective dyes, the possible side effects of these exogenous agents must be comprehensively evaluated to ensure physiological validity of the tissue preparation.

One such technique that operates at high spatial resolution is voltage-sensitive dye imaging (VSDI), used to capture real-time, two-dimensional changes in transmembrane potential using membrane-bound molecules containing a chromophore that changes its absorbance or fluorescence spectrum depending on the local electrical field. These changes in absorbance or fluorescence, which take place on a submicrosecond timescale, are recorded by fast-capture video cameras with sampling rates that can exceed 1 kHz; thus the technique acts like a "two-dimensional electrode". Like other imaging techniques operating at this scale, an exogenous agent must be added to the tissue to visualize activity. This has the potential to lead to several undesired effects: *1*) direct pharmacological side effects (i.e., interactions of the dye with membrane-bound receptors and channels) that change the neurophysiological characteristics of the system; *2*) indirect cumulative effects on the physiology of the preparation such as phototoxicity due to free radical formation caused by the exposure of the dye molecules to high-energy light; and *3*) restrictions placed on overall imaging time if the agent becomes washed out of the tissue and/or the dye is "bleached". It has been reported that these challenges, together with the pursuit of improved SNRs, have slowly been overcome, especially for more recent VSDs such as di-4-ANEPPS and RH-1691 (Loew 1996; Loew et al. 1992; Schaffer et al. 1994; Shoham et al. 1999; Slovin et al. 2002).

Nevertheless, the absence of pharmacological side effects in RH-1691, in particular, has rarely been confirmed and has only ever been partly assessed for in vivo preparations in rodents, even though it is known that properties of dyes can differ considerably from preparation to preparation (e.g., Loew 1996). Furthermore, since the first use of RH-1691 to demonstrate cortical dynamics in visual cortices of awake monkeys (Slovin et al. 2002), the concentrations used have increased gradually from 0.1–0.3 mg/ml (Slovin et al. 2002) to 1 mg/ml (Borgdorff et al. 2007; Civillico and Contreras 2005; Ferezou et al. 2006, 2007) and 2 mg/ml (Lippert et al. 2007), without any re-assessment of potential side effects at higher concentrations. The situation is the same for di-4-ANEPPS, which has been used primarily within neuroscience for in vitro preparations (Collins et al. 2007; Mann et al. 2005; Tominaga et al. 2000); we are not aware of any investigations of its use and evaluation for in vivo preparations apart from our own previous work (Devonshire et al. 2010a, b). Furthermore, a recent study (Mennerick et al. 2010) has reported strong potentiation of $GABA_A$ receptor function in vitro after application of RH-1691 as well as di-4-ANEPPS. Therefore, in the current

Address for correspondence and present address: I. M. Devonshire, Univ. of Nottingham, School of Biomedical Sciences, Medical School, Queen's Medical Centre, Nottingham, NG7 2UH, UK (e-mail: ian.devonshire@nottingham.ac.uk).

study, we have investigated and compared the existence of pharmacological side effects associated with RH-1691 and di-4-ANEPPS to assess their suitability for in vivo studies. Our own preliminary investigations of di-4-ANEPPS (Devonshire et al. 2010b) did not indicate any adverse effects and will be reported here in more detail. The current study used rats with an intact dura with commonly used dye concentrations of 1 mg/ml (1.7 mM) for RH-1691 (Borgdorff et al. 2007; Civillico and Contreras 2005; Ferezou et al. 2006, 2007) and 0.1 mg/ml (0.2 mM) for di-4-ANEPPS (Collins et al. 2007; Mann et al. 2005; Tominaga et al. 2000).

We also report an evaluation of a heartbeat-associated brain-pulsation artifact (BPA) removal paradigm, originally introduced by Jian-Young Wu and colleagues (Lippert et al. 2007; Ma et al. 2004) for use with the recording of spontaneous and epileptic cortical activity. Compared with traditional methods of removing the BPA (Grinvald et al. 1984; Slovin et al. 2002) by subtracting alternating sweeps of stimulus and no-stimulus recordings that are time locked to the electrocardiogram [i.e., the subtraction method (SM)], this new approach uses segments of data centered on the heartbeat to create an artifact template, which is then subtracted [i.e., the template-based method (TBM)]. Use of the TBM halves the overall imaging time and reduces potential phototoxic effects by removing the need to acquire and subtract the no-stimulus trials. To the best of our knowledge, the algorithm has not been applied previously to short stimulus-evoked trials (i.e., 2–3 s) such as those used in this study and therefore, if successful, could be applied to other such investigations of cortical sensory function. Indeed, VSDI is used increasingly in chronic rodent preparations to image cortical sensory function in behaving and even freely moving animals (Ferezou et al. 2006, 2007) and has been shown to offer a promising preparation for long-term studies in nonprimates without durectomy (Lippert et al. 2007).

Finally, we assessed and compared *1*) noise levels associated with brain pulsation and *2*) the shot noise of both dyes, which stems from statistical fluctuations of photons emitted by the dye molecules (Waggoner and Grinvald 1977) following successful BPA removal with the TBM. Previous reports (Civillico and Contreras 2005; Lippert et al. 2007; Shoham et al. 1999) suggested that the noise level for RH-1691 is smaller with respect to the BPA level as well as the shot noise, thus providing a better SNR. Explicit removal of the BPA by means of the TBM artifact correction allowed us to disentangle the two noise components and compare them separately for both dyes. Additionally, we conducted imaging with both dyes at comparable levels of overall measured absolute fluorescence, thus being able to directly compare the shot noise levels of the two dyes on the same scale.

In summary, the current study pursued three major goals. First, we were to assess and re-assess potential pharmacological side effects of using the dyes di-4-ANEPPS and RH-1691 in an in vivo rodent somatosensory cortex preparation, especially in light of the recent study by Mennerick and colleagues (2010). This assessment was performed by comparing evoked responses before, during, and after dye application. Secondly, we were to evaluate a template-based BPA removal algorithm proposed by Wu and colleagues (Lippert et al. 2007; Ma et al. 2004), extending the approach to short trials of 2.4 s containing evoked activity, and assess its applicability to di-4-ANEPPS, which was not reported previously. Our final goal was to compare the noise levels of both dyes with respect to the two dominating noise components in in vivo VSDI—the BPA and the shot noise—and examine implications regarding the SNR of both dyes.

MATERIALS AND METHODS

Animals and surgical procedures. Female Wistar-Han rats (Hsd-Han:WIST, Harlan Laboratories, Bicester, UK; $n = 12$), weighing between 210 and 260 g, were used; seven animals were used for the evaluation of the dye RH-1691 and five for the evaluation of the dye di-4-ANEPPS. Animals were kept on a 12-h dark/artificial-light cycle in an open-system holding room at a temperature of 22°C and a humidity of 55%. Food (RM3P, Special Diet Services, Witham, UK) and water were available ad libitum. The experiments described were approved by the local university ethical committee, and all procedures were performed with Home Office approval under the Animals (Scientific Procedures) Act 1986.

Rats were anesthetized with urethane (1.15 g/kg) and chloral hydrate (0.16 g/kg) and transferred to a stereotaxic frame (David Kopf Instruments, Tujunga, CA). Respiratory and cardiovascular parameters were recorded throughout surgical and experimental procedures. Rate and depth of respiration were recorded using a custom-built monitor based around an accelerometer-integrated circuit (Devonshire et al. 2009). Heart rate was recorded via single-strand copper ECG recording leads inserted subcutaneously behind each forelimb and connected to a custom-built ECG processing unit. A craniotomy was performed over the primary somatosensory cortex at the following approximate stereotaxic coordinates: anterior–posterior = 1–5 mm; medial–lateral = 4–8 mm. A single trepanne hole (~1 mm in diameter) was drilled in the left frontal bone into which a short loop-tipped silver-wire electrode (0.2 mm in diameter; Intracel, Royston, Hertfordshire, UK) was inserted to act as a reference electrode. An imaging chamber comprising a 3-mm section of a disposable 5-ml syringe (Becton Dickinson, Oxford, UK) was cemented in place around the craniotomy using dental cement (DuraLay, Reliance Dental Manufacturing, Worth, IL).

Sensory stimulation. All whiskers on the left-hand side of the snout were trimmed apart from *whisker C2*. The remaining whisker was stimulated 3 mm from its base by a 26G hypodermic needle attached to a piezoelectric wafer (PL122.11, Physik Instrumente, Harpenden, UK). Displacement of the wafer was produced by applying an electrical potential across it (10 V for 20 ms) to give ~2 mm of movement in a caudal direction. Within each stimulation trial, whiskers were deflected at 2 Hz; analyses in this study focused on the neural response to the first stimulus only.

Staining and optical imaging. Staining of the barrel cortex was either done with the blue oxonol dye RH-1691 (Optical Imaging, New York, NY) at a concentration of 1 mg/ml (=1.7 mM) (Borgdorff et al. 2007; Civillico and Contreras 2005; Ferezou et al. 2006, 2007) in artificial cerebrospinal fluid (aCSF; containing in mM: NaCl 124, KCl 3.7, $NaHCO_3$ 26, $CaCl_2$ 2, $MgSO_4$ 1.3, KH_2PO_4 1.3, glucose 10) or with the red styryl dye di-4-ANEPPS (Invitrogen, Paisley, UK) at a concentration of 0.1 mg/ml (=0.2 mM) (Collins et al. 2007; Mann et al. 2005; Tominaga et al. 2000) in 48.1% FBS, 48.1% aCSF, 3.6% DMSO, and 0.2% Chremophor EL. The dura was kept intact for both dye preparations, but contrary to the staining protocol introduced by Lippert and colleagues (2007), who also performed imaging without durectomy, we found sufficient staining without drying the dura before application of the dyes.

RH-1691 was applied to the surface of the brain for 90 min (Civillico and Contreras 2005; Lippert et al. 2007). We filled the imaging chamber with ~300 μl of the dye solution and reapplied fresh solution every 30 min. After dyeing, unbound dye was washed out for >15 min before imaging started. For data acquisition with the blue dye, excitation light was band-pass filtered at 632 ± 11 nm, and emitted light (>664 nm) passed through a 655-nm high-pass filter.

di-4-ANEPPS was applied to the cortical tissue in the same way, but preliminary investigations revealed that a period of 60 min resulted in sufficient staining of cortical tissue for the in vivo preparation with reapplication after 30 min. After the chamber was drained of dye, manual washing out of unbound dye took place for ~15 min. To keep the timing constant for both dyes, we started imaging ~105 min after application of di-4-ANEPPS, equivalent to the time taken with RH-1691 staining and washout. For data acquisition with the red dye, the cortex was illuminated with light band-pass filtered at 530 ± 10 nm, and emitted light passed through a 590-nm high-pass filter.

All recordings were performed with the imaging chamber filled with aCSF. To avoid scattering of light due to washed-out unbound dye molecules, the aCSF was exchanged with fresh aCSF every 30 min. Optical imaging data acquisition was done with a complementary metal oxide semiconductor imaging system (Ultima, BrainVision, Tokyo, Japan) with an array of 100 × 100 sensors. In each trial, frames were recorded at a sampling rate of 500 Hz for 2.4 s with a prestimulus period of 0.5 s. A brief initial imaging session (consisting of five stimulation trials) was performed to locate the maximal site of activation and position the imaging camera appropriately.

Electrophysiology. EEG and somatosensory-evoked potential (SEP) recordings for three RH-1691 and five di-4-ANEPPS experiments were made with a single platinum–iridium bipolar electrode (25 μm diameter; FHC, Bowdoin, ME). The electrode was initially placed between the two branches of the medial cerebral artery, and the location was further optimized using SEPs from C2 whisker stimulation as feedback. Post hoc estimation of the distance of the electrode to the center of activation at C2, as obtained in the VSDI, revealed no significant difference between the dyes: 15.2 pixels ± 7.6 pixels (SE) for RH-1691 and 21.8 pixels ± 8.4 pixels for di-4-ANEPPS.

In four experiments with RH-1691, EEG and SEP recordings were conducted with a short loop-tipped silver-wire electrode (0.2 mm in diameter; Intracel) placed at the caudal border of the craniotomy. In these experiments, the distance of the tip of the silver-wire electrode to the center of activation at C2 amounted to 44.7 pixels ± 6.5 pixels.

The EEG/SEP signal was processed via a NeuroLog headstage preamplifier and filter module (NL100AK, NL104A, NL125, Digitimer, Welwyn Garden City, UK), high-pass filtered with 1 Hz half amplitude cutoff, and displayed in Spike2 software via a Micro CED 1401 data acquisition unit (Cambridge Electronic Design, Cambridge, UK).

Recording protocol. To assess pharmacological side effects of the dyes, two recording protocols were used. Direct comparison of the two dyes (RH-1691: $n = 3$; di-4-ANEPPS: $n = 5$) was obtained using the EEG/SEP setup with the bipolar electrode. Here, we recorded 90 SEPs over a period of 90 min as a baseline prior to applying the dye. Importantly, the pre-dye baseline recording started after all surgical procedures were completed, and the whole preparation was set up, i.e., with the imaging chamber mounted and filled with aCSF. Stimulation, as described above, was applied with intertrial intervals (ITIs) of 60 s, and SEP recordings continued during the whole staining period and washout of the dye. Optical imaging was conducted concurrently with electrophysiological recordings once staining was complete, and unbound dye was washed out. For every animal, a total of 4 h was recorded poststaining with interleaved stimulation/no-stimulus (i.e., optical imaging and electrophysiological recording without whisker stimulation) trials recorded every 30 s; thus the ITI between stimulation trials amounted to 60 s, as during the baseline and staining period.

To obtain a sound estimate of the pharmacological side effects of RH-1691 on evoked potentials, we included additional data ($n = 4$) from a second set of experiments where the EEG/SEP was recorded with a silver-wire electrode placed at the caudal border of the craniotomy. Again, SEP recording started after all surgical procedures were completed, and the whole preparation was set up. In these experiments, on average, 20 SEPs were recorded before dyeing, and 30 SEPs were recorded, distributed over the whole staining period. After dyeing was completed, optical imaging was conducted concurrently with electrophysiological recordings for 3.75 h on average (range: 2.25–6.5 h); data of up to 3 h of recording will be reported here. ITIs amounted to 60 s, but differently from the recordings with the bipolar electrode, recordings were obtained in blocks of 10 trials interleaved with a break of 5 min; that is, 40 trials/hour were recorded during imaging. As in the experiments with the bipolar electrode setup, an interleaved stimulation/no-stimulus trial recording scheme was used during optical imaging; each stimulation trial was followed by a no-stimulus trial after 30 s.

The reason for recording no-stimulus trials was to compare the standard heartbeat-pulsation artifact removal approach (Grinvald et al. 1984; Slovin et al. 2002) with the heartbeat-pulsation artifact removal algorithm introduced by Jian-Young Wu and colleagues (Lippert et al. 2007; Ma et al. 2004) directly. Both stimulation and no-stimulus trials were triggered by the R-wave of the ECG, enabling subtraction of corresponding no-stimulus trials from the preceding stimulation trial (Grinvald et al. 1984; Slovin et al. 2002).

Data analysis. All data analyses were performed with custom-written routines in MATLAB (MathWorks, Natick, MA); statistical testing was conducted using SPSS 15.0 (SPSS, Chicago, IL). Three main analyses were performed: *1*) assessment of pharmacological side effects of the VSDs by evaluating changes in SEP response amplitudes and spectral content of the EEG before, during, and after staining with VSDs, as well as comparing spatiotemporal characteristics of the evoked VSDI responses; *2*) comparison between the two BPA removal algorithms with a special focus on the evaluation of applicability of the TBM artifact removal algorithm to di-4-ANEPPS; *3*) examination and comparison of shot noise and BPA levels for both VSDs.

SEPs. It was expected from previously published results that two large response components would be observable in the SEP data: an initial positive deflection (P1), followed by a negative deflection (N1) (Di and Barth 1991). The peak-to-peak amplitude between these response components was taken as our overall measure of sensory responsiveness, acquired before, during, and after cortical staining. SEP data were band-pass filtered at 1–250 Hz.

Ongoing EEG activity and assessment of anesthetic depth. Small fluctuations in anesthetic depth are common with most anesthetic regimens and are often observed with urethane anesthesia, the anesthetic used in the current study (Angel 1991; Friedberg et al. 1999). To assess changes in the level of anesthesia and associated changes in spontaneous activity—and to ensure anesthetic depth was comparable between both dye preparations—we analyzed the spectral content of the EEG around the sensory stimulus presentations as described in Devonshire et al. (2010b). In short, a fast-Fourier transform (FFT) was calculated for every trial, and the mean power frequency was obtained. Mean power frequencies above 2.5 Hz were identified as "light" levels of anesthesia, mean power frequencies below 1 Hz as "deep" levels of anesthesia, and all other mean power frequencies were categorized as "moderate" levels of anesthesia. Note that all three anesthetic levels described here are actually sublevels of an anesthetic state deemed to be appropriate for surgery. Data used for the analysis of dye effects upon spontaneous EEG activity among animals are from the five di-4-ANEPPS experiments and from five RH-1691 experiments (three experiments with the bipolar electrode and two experiments with the silver-wire electrode, where >30 min of baseline recordings allowed a sound estimate of the distribution of different anesthetic states).

VSDI. Recording of the imaging data was controlled by the BrainVision MiCAM software (BrainVision), and raw imaging data were converted to fractional change in fluorescence by dividing the change in fluorescence by the background fluorescence ($\Delta F/F$). The $\Delta F/F$ data were used for all analyses. Imaging data were high-pass filtered with 1 Hz half amplitude cutoff. Temporal information was extracted from the imaging data by using a circular region of interest (ROI) centered on the pixel with maximum activation within the first 20 ms after stimulation (Devonshire et al. 2010a, b). We have shown previously

that with the use of this criterion, the ROI was contained entirely within the C2 barrel, corresponding to the whisker that was stimulated (Devonshire et al. 2010b).

Removal of the BPA. The dominating physiological noise in almost all in vivo VSDI recording setups is the pulsation of the vessels and brain tissue. This pulsation is caused by a pulse wave arising from the contraction of the left ventricle of the heart during systole. Even though it has been shown that this artifact is reduced significantly when using blue dyes (Civillico and Contreras 2005; Lippert et al. 2007; Shoham et al. 1999), due to their spectral properties being farther away from the spectrum of hemoglobin, the pulsation still causes a considerable artifact in fluorescence recordings with RH-1691 as well as di-4-ANEPPS. For both dyes, the artifact can be up to several-fold larger than the signal of interest (e.g., Civillico and Contreras 2005; Lippert et al. 2007; Shoham et al. 1999).

Recently, a new approach for the removal of the heartbeat-associated pulsation artifact for long sweeps of spontaneous and epileptic cortical activity was described by Jian-Young Wu and colleagues (Lippert et al. 2007; Ma et al. 2004), and we implemented and evaluated this approach for shorter trials containing evoked activity with a focus on di-4-ANEPPS, as described in the next paragraph. Following Lippert and colleagues (2007), we will also call the artifact BPA. In short, this approach makes use of two facts: *1*) the pulsation artifact is time locked to the heartbeat and therefore to the ECG, and *2*) it is very stereotypical, and thus an average pulsation artifact (as a template) can be created and subtracted successfully from the raw data.

The steps implemented for the BPA removal following Ma et al. (2004) and Lippert et al. (2007) are reviewed briefly: *1*) for each optical recording, the peak latencies of the R-waves in the concurrently recorded ECG were determined; *2*) for each sensor, the ΔF/F time series were cut into segments around the determined R-waves, and length of the segments was chosen to be ±1.5 times the average time elapsing between two consecutive R-waves in the ECG; *3*) after segmentation, segments were detrended linearly to account for slow drifts, aligned with respect to the R-waves and averaged, thus creating an average BPA (BPA template); *4*) the BPA template then was realigned, corresponding to the original R-wave latencies, and segments were concatenated; to avoid sudden steps in the concatenated data, concatenation was done using a linear-weighted transition from each R-wave to the neighboring R-waves; and *5*) the concatenated pulsation artifact was then subtracted from the raw ΔF/F time series. Furthermore, to overcome contamination of the average BPA by the evoked responses, data points in the time window of the evoked response (i.e., from 0 to 50 ms after each stimulation) were replaced by random data points. The root mean square (RMS) of the random data points was matched to the dark noise level of the camera system and the shot noise level of the corresponding background fluorescence of that pixel. It is important to note that compared with the standard BPA removal (Grinvald et al. 1984; Slovin et al. 2002), this new approach halves the illumination time, since no-stimulus trials are not needed. The code for the heartbeat-pulsation artifact removal will be provided upon request.

Since the heart rate is very stable, and the BPA clearly dominates the VSDI signal in a number of pixels, an effective method to verify successful removal of the BPA is required. Removal was demonstrated by showing the elimination of power in the signal at the heartbeat frequency and associated harmonics but only these frequencies in a FFT of the fluorescence data. FFT was obtained pixel wise for the VSDI signal and averaged, aligned to the heartbeat frequency to compare the reduction of power at the heart rate for the raw data vs. the two artifact removal methods. Analysis focused on the 20% of all imaged pixels showing the strongest BPA by means of the RMS of the BPA.

Noise estimation and comparison. We compared noise characteristics of RH-1691 and di-4-ANEPPS for two dominating noise components found in in vivo VSDI: the BPA and the shot noise relative to the background fluorescence. The BPA was quantified by calculating the RMS of the BPA template for each pixel and trial and subsequently averaging over all 240 trials for each animal. To quantify the shot noise, the RMS of the ΔF/F data of the 100 ms prior to the first sensory stimulus (baseline) after the TBM artifact correction was calculated (Civillico and Contreras 2005). It should be noted that by means of the TBM BPA artifact correction, we were able to disentangle the BPA and shot noise and obtain nonconfounded estimates for these two noise components.

RESULTS

Evaluation of pharmacological side effects using SEP recordings. Figure 1*A* illustrates the grand average SEP responses for the directly comparable di-4-ANEPPS ($n = 5$) and RH-1691 ($n = 3$) experiments recorded with a bipolar electrode during different stages of the experiments: 1.5 h of baseline recording (before application of the dye), 1.5 h of staining, the first 1.5 h of imaging, and the last 1.5 h of imaging. Baseline conditions between the two groups were comparable, as indicated by the similarity in baseline SEP responses (0-lag cross-correlation between the di-4-ANEPPS and RH-1691 signal before dyeing: $r = 0.876$, $P < 0.01$), thus also proving that our electrode placement procedure was successful. During application of di-4-ANEPPS, the SEP response increased but returned to the pre-dye size when imaging began (0-lag cross-correlation between the signal before and after dyeing: $r = 0.989$, $P < 0.01$). In contrast, the SEP response from the cortex stained with RH-1691 increased progressively over time and showed considerably different characteristics during imaging compared with the baseline recording: when imaging started, the SEP was not correlated to the baseline SEP anymore (0-lag cross-correlation between the SEPs before and after dyeing: $r = -0.029$, $P > 0.5$).

Figure 1*A* also provides a very similar picture from four additional experiments with RH-1691, where SEPs were recorded with a silver-wire electrode. The 0-lag cross-correlation between the signal before and after dyeing was essentially zero ($r = 0.062$, $P > 0.3$), indicating a substantial qualitative change in the SEP waveform reproducing the change observed using the bipolar electrode.

Statistical analyses focusing on the P1–N1 peak-to-peak amplitude in response to whisker stimulation underscored these observations. The development of the P1–N1 amplitude over the course of the experiments with the bipolar electrode is shown in Fig. 1*B*. Fifteen consecutive whisker stimulations were averaged (representing a period of 15 min) to illustrate the change in response over time. At baseline, repeated measures ANOVA (rmANOVA) with the factors dye × time (six 15-min bins representing 1.5 h of baseline recording) revealed no significant differences between the two dyes ($F = 5.948$, $P > 0.05$), as well as no effect of time ($F = 1.004$, $P > 0.05$). Thus the initial conditions for di-4-ANEPPS and RH-1691 were comparable and stable. In contrast, during dyeing, a significant difference between the two dyes ($F = 12.983$, $P < 0.05$) as well as a highly significant effect of time ($F = 39.037$, $P < 0.01$) and a highly significant interaction ($F = 8.754$, $P < 0.01$) were observed, reflecting the increase of P1–N1 amplitude for both dyes, as well as the disproportionately steeper increase of the P1–N1 amplitude during dyeing with RH-1691. Furthermore, comparing the baseline with the first 1.5 h of imaging also revealed a highly significant difference between

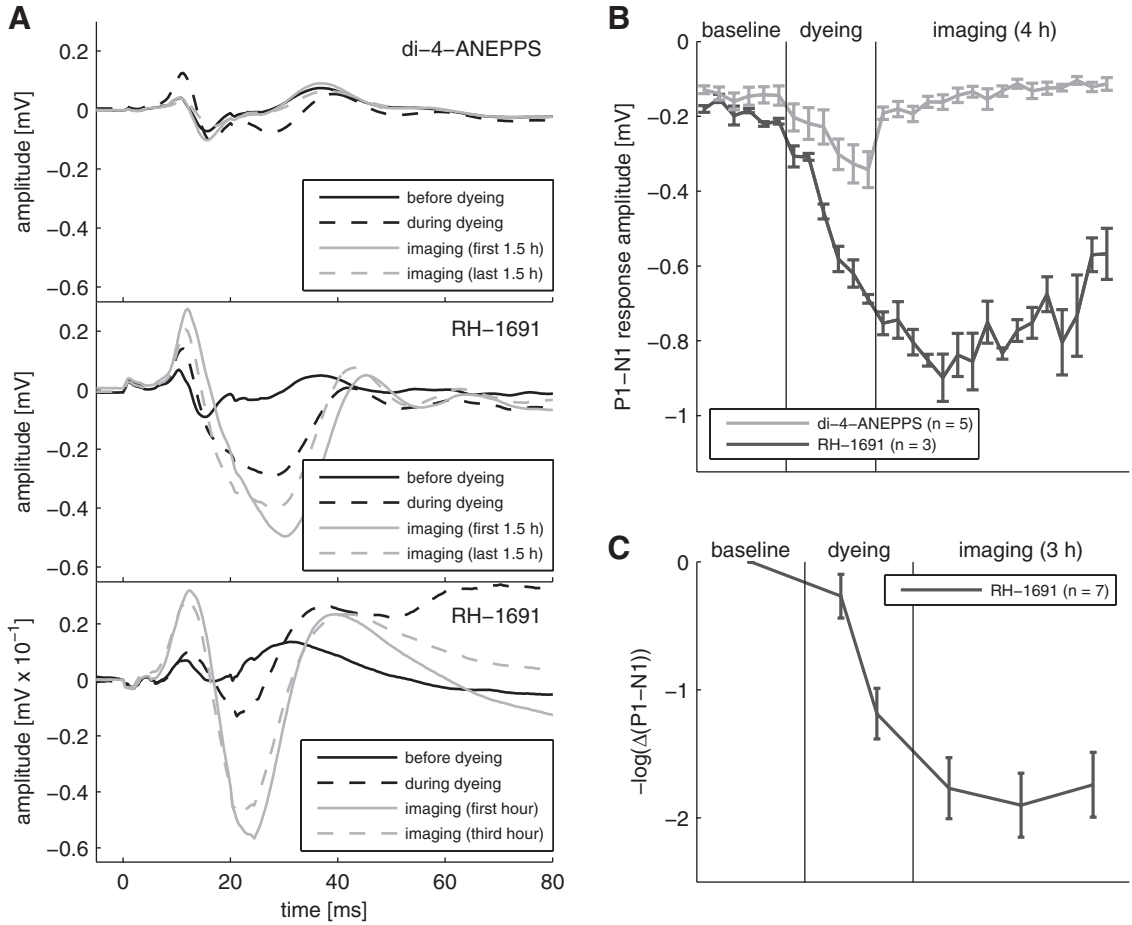

Fig. 1. Change in somatosensory-evoked potential (SEP) response profiles over the course of the experiment. *A*: grand average SEP responses for di-4-ANEPPS ($n = 5$, *top plot*) and RH-1691 experiments ($n = 3$, *middle plot*) recorded with a bipolar electrode, as well as for additional RH-1691 experiments ($n = 4$, *bottom plot*; note the different scaling) recorded with a silver-wire electrode at different stages of the experiment. *B*: initial positive–negative deflection (P1–N1) peak-to-peak amplitudes over the experiments conducted with the bipolar electrode; each point represents an average over 15 consecutive whisker stimulations, spanning a period of 15 min. *C*: aggregation of data across all RH-1691 experiments ($n = 7$), indicating that the increased SEP response due to application of RH-1691 is highly systematic. Error bars indicate ± 1 SE; baseline refers to SEP recordings before application of the dye.

dyes ($F = 196.480$, $P < 0.01$), as well as a highly significant effect of time ($F = 93.956$, $P < 0.01$) and a highly significant interaction ($F = 79.414$, $P < 0.01$). Post hoc contrast revealed that there was no effect of time for di-4-ANEPPS (rmANOVA with factor time: $F = 1.606$, $P > 0.1$). Thus the increase in response during dyeing with di-4-ANEPPS had indeed returned to baseline levels when imaging started. Furthermore, statistical comparison of the baseline to the last 1.5 h of imaging revealed the same picture: a highly significant difference between dyes ($F = 88.998$, $P < 0.01$), as well as a highly significant effect of time ($F = 34.049$, $P < 0.01$) and a highly significant interaction ($F = 40.461$, $P < 0.01$). Importantly, the post hoc contrast for di-4-ANEPPs did again show no effect of time ($F = 0.847$, $P > 0.1$), indicating that also, the last 1.5 h of imaging with di-4-ANEPPS were comparable with the initial baseline SEP recordings.

A clear and systematic increase in SEP amplitude was also observed in the four additional experiments using RH-1691 with the alternative electrophysiological recording setup (Fig. 1*A*). Figure 1*C* provides the average logarithmic transformed changes of SEP amplitudes relative to baseline of all seven RH-1691 experiments. Transformation of data previous to aggregation was necessary to account for the different scaling of the SEP responses as a consequence of the differing recording setups (compare scaling in Fig. 1*A*; the silver-wire electrode was three times farther away from the center of the evoked response) and to stabilize variance. Nevertheless, the same overall picture was also found in the statistical analyses using the raw, untransformed values as will be reported below, indicating that reported effects are not due to transformation of the data.

Figure 1*C* indicates that the increased SEP amplitude is consistent over seven experiments (across different recording conditions). rmANOVA revealed a highly significant effect of time ($F = 19.524$, $P < 0.001$); importantly, this was also observed in a rmANOVA for the raw, untransformed data ($F = 8.510$, $P < 0.001$). One-sample *t*-test contrasts (pre-dye baseline vs. 1st, 2nd, and 3rd h of imaging) indicated that the significant effect of time was due to significantly larger SEP amplitudes after dyeing compared with the pre-dye baseline recordings and that this effect lasted for at least 3 h after the dyeing solution was removed ($t_{pre\ vs.\ 1st\ h} = 7.417$, $P < 0.001$; $t_{pre\ vs.\ 2nd\ h} = 7.596$, $P < 0.001$; $t_{pre\ vs.3rd\ h} = 6.884$, $P < 0.001$); contrasts for the raw data revealed the same picture ($t_{pre\ vs.\ 1st\ h} = 2.903$, $P < 0.05$; $t_{pre\ vs.\ 2nd\ h} = 2.950$, $P < 0.05$; $t_{pre\ vs.3rd\ h} = 2.904$, $P < 0.05$). Thus the effect of the dye RH-1691 on the P1–N1 amplitude is consistent across several experiments.

Table 1. *Distribution of anesthetic levels (deep, moderate, light) across the different periods (baseline, dyeing, imaging) of the experiment*

	di-4-ANEPPS ($n = 5$)			RH-1691 ($n = 5$)		
	Baseline	Dyeing	Imaging	Baseline	Dyeing	Imaging
Deep	14.7 ± 2.8	14.9 ± 3.1	18.8 ± 4.9	14.8 ± 4.1	22.8 ± 9.8	17.7 ± 4.1
Moderate	66.2 ± 4.1	72.2 ± 3.7	68.2 ± 5.1	67.6 ± 4.6	68.6 ± 7.9	70.3 ± 2.4
Light	19.1 ± 5.3	12.9 ± 6.6	13.0 ± 3.9	17.6 ± 8.2	8.6 ± 3.4	12.0 ± 3.6

Values are relative proportion of time in percent ±1 SE.

Assessment of the influence of the dyes on the background EEG. Importantly, when assessing the level of anesthesia over time, we did not find any significant change of the relative proportions of the three different surgical anesthetic levels over the course of the experiment ($F = 0.393$, $P > 0.5$). Table 1 indicates that the animals spent the major amount of time in a moderate level of anesthesia. Furthermore, no difference between the two dyes with respect to the relative proportion of anesthetic levels was found ($F = 1.589$, $P > 0.2$). Thus systematic changes in the level of anesthesia over time can be ruled out as a confounding factor responsible for the change of the SEPs, and equally, differences in the levels of anesthesia can be ruled out as being responsible for the observed differences between the two dyes. Figure 2 shows the spectral content of the EEG across the three different levels of surgical anesthesia and the two dyes. It can be seen that from the baseline to the imaging period, no apparent systematic differences in the frequency content of the EEG up to 15 Hz can be seen. Thus contrary to the evoked activity, the ongoing, spontaneous EEG does not seem to have been affected by either dye.

Post hoc analysis of SEP changes of the experiments conducted with the bipolar electrode setup, restricted to trials that could be identified as having been recorded within a moderate state of anesthesia, essentially revealed the same picture as reported above (Fig. 1*A*). A significant increase of the P1–N1 amplitude from baseline to the dyeing period was found for both dyes (di-4-ANEPPS: $t = 3.834$, $P < 0.05$; RH-1691: $t = 19.176$, $P < 0.01$). Whereas for di-4-ANEPPS, the P1–N1 amplitude returned to the baseline level ($t = 0.194$, $P > 0.5$), RH-1691 also expressed for the imaging period a highly significant increase of the P1–N1 amplitude compared with baseline ($t = 12.454$, $P < 0.01$).

Evaluation of BPA removal. Since the template-based BPA removal method was evaluated thoroughly by Wu and colleagues for RH-1691 (Lippert et al. 2007; Ma et al. 2004), we focused the evaluation of the BPA removal on di-4-ANEPPS. Figure 3 illustrates the outcome after applying each of the two BPA removal algorithms—the TBM and the SM—to a single imaging trial of di-4-ANEPPS. Figure 3*A* shows the raw ΔF/F signal, the fluorescence signal after TBM artifact correction, and after subtracting a subsequently recorded trial that was time-locked to the heartbeat (SM) from one ROI. Marked perturbations in the raw signal (i.e., the BPA), time locked to the ECG R-wave, can be discerned and appear to be removed successfully by the TBM artifact correction (Fig. 3*B*). The most effective method to verify successful removal of the BPA is by showing the elimination of power in the signal at the heart rate and associated harmonics, but only these frequencies, in a FFT of the fluorescence data (Fig. 3*C*). It can be seen from the FFT shown in Fig. 3*C* that the TBM most successfully removed the power at the heartbeat frequency (~8 Hz) and its harmonics (~16 and ~24 Hz), while leaving all other frequencies unaltered.

Before quantitatively comparing the TBM with the SM artifact correction for the complete data set, two further pitfalls of the SM can be highlighted with the single-trial data shown. Figure 3*B* provides the signal that was removed from the raw data by means of the TBM (concatenated template) as well as the SM (subsequently recorded trial with no sensory stimula-

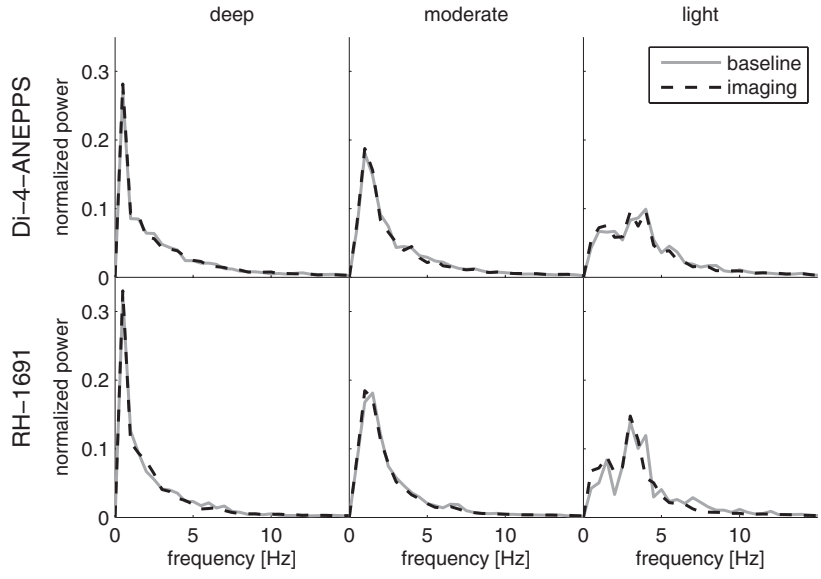

Fig. 2. Average normalized power spectra of the 3 different levels of surgical anesthesia for the 2 different dyes. Note that only experiments were included that ensured a sufficient amount of data at the pre-dyeing baseline (i.e., >30 min of recordings), resulting in data from 5 di-4-ANEPPS and 5 RH-1691 experiments shown here. No systematic statistical differences between the baseline and imaging periods in the spectra up to 100 Hz were found, indicating that neither dye affected the ongoing EEG activity.

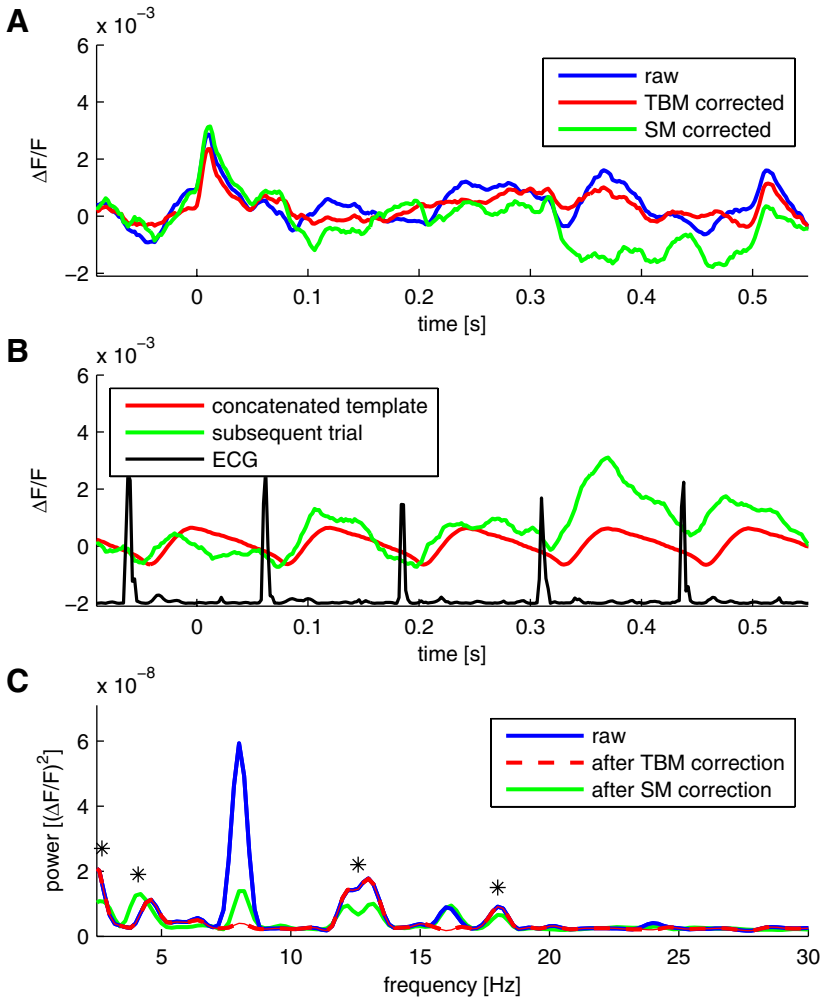

Fig. 3. Illustration of the outcome of applying the 2 brain-pulsation artifact (BPA) removal methods to the region of interest (ROI) of a single di-4-ANEPPS trial. *A*: comparison of the raw data (blue trace) with the data after either artifact removal method [template-based method (TBM): red trace; subtraction method (SM): green trace]. *B*: signals (i.e., BPA) that were subtracted from the raw data to obtain the corrected data: concatenated template (red trace) and subsequent trial (green trace). Plotted on top is the ECG recording from this trial (black trace). *C*: fast-Fourier transform (FFT) spectra for the raw as well as corrected data. Note that the TBM selectively removes power at the heartbeat frequency (~8 Hz) and its harmonics (i.e., ~16 and ~24 Hz), whereas the SM also changed the spectrum at frequencies not associated with the heart rate (indicated by asterisks). ΔF/F, change in fluorescence divided by background fluorescence.

tion). First, it can be seen that the signal that was subtracted out using the SM was shifted slightly compared with the concatenated BPA template. This is due to slight shifts or irregularities in the heart rate. Whereas the TBM artifact correction makes use of the ECG for explicitly aligning the BPA template to the heartbeat, the SM is dependent on perfectly stable heartbeats. In reality, the heartbeats in anesthetized rats are very stable but not perfectly so. This is also reflected in the FFT of the SM: in contrary to the TBM, the FFT of the SM corrected data contains a residual peak at the heart rate (Fig. 3*C*). Secondly, it can be seen that by subtracting a subsequent no-stimulus trial, spontaneous activity within this subsequent trial has been subtracted from the stimulus trial in addition to the BPA, resulting in prominent changes in the fluorescence signal (e.g., the pronounced negativity from 0.3 to 0.5 s in Fig. 3*A*). This is also reflected in the FFT by changes in power at frequencies not associated with the BPA (see Fig. 3*C*).

The FFT findings are summarized in Fig. 4. Figure 4*A* subsumes for all di-4-ANEPPS experiments ($n = 5$) the mean power distribution relative to the heart rate; to focus on the pixels that were affected strongest by the BPA, analyses were done for the upper quintile of all pixels in terms of RMS of the BPA. Exactly the same picture as described for the single trial emerged. Both artifact correction approaches are very powerful in reducing the BPA: there is a significant reduction of the BPA-related power after either artifact removal method ($t = 3.1598$, $P < 0.05$, for raw vs. SM corrected data; $t = 3.2409$, $P < 0.05$, for raw vs. TBM corrected data). The mean power values at the heart rate are plotted in Fig. 4*B* (note that the scaling for the raw signal power is 10-fold compared with the scaling after artifact correction). However, in addition to the considerable reduction in BPA-related power, the TBM does significantly reduce the BPA-related artifact further ($t = 3.5402$, $P < 0.05$), pointing to the fact that there remains some residual power at the heart rate when using the SM artifact correction. By applying the TBM artifact correction, there is no difference between the power 2 Hz above the heart rate (used as a proxy for the expected artifact free power at the heart rate) and the power at the heart rate ($t = 2.3161$, $P > 0.05$), indicating that in terms of the frequency content, the BPA is removed successfully by the TBM artifact correction applied to single-trial data.

Two further observations are noteworthy. First, as suggested in the literature, red dyes, such as di-4-ANEPPS, seem to show a stronger BPA, as reflected in the nearly fivefold-stronger power of di-4-ANEPPS compared with RH-1691 at the heartbeat frequency (Fig. 4*B*). Secondly, after artifact removal and at frequencies not related to the BPA (e.g., 2 Hz above the heart rate), both dyes show equal power—the power values of RH-1691 lie well within the mean ± 1 SE of the di-4-ANEPPS power values (Fig. 4*C*). This indicates that for both dyes,

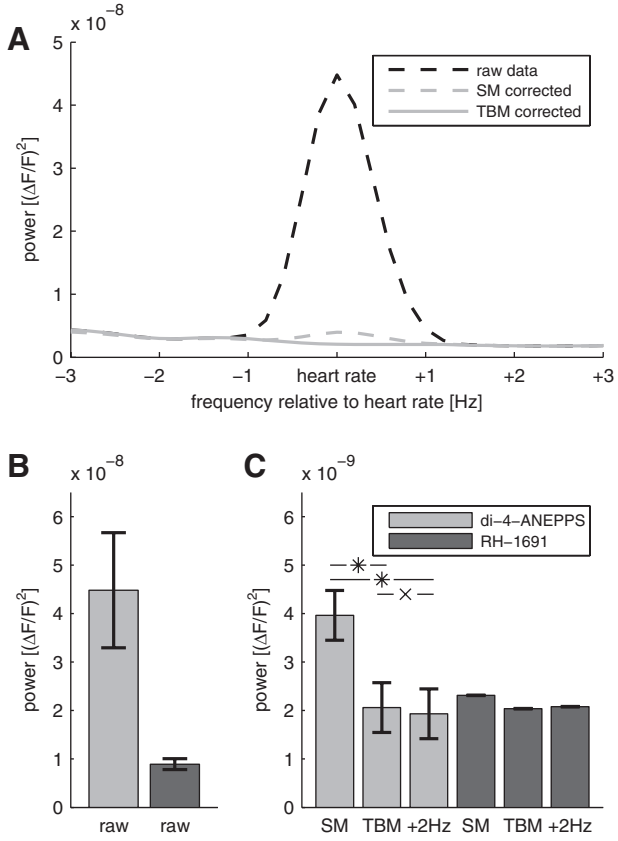

Fig. 4. Summary and evaluation of the BPA removal methods by means of FFT analysis. *A*: average FFT spectrum aligned to the heart rate for all di-4-ANEPPS experiments ($n = 5$) before (black dashed line) and after (gray lines) artifact removal. *B* and *C*: average power at the heartbeat frequency for di-4-ANEPPS and RH-1691 before (*B*) and after (*C*) artifact removal; error bars indicate ±1 SE. Note that the scaling in *B* is 10-fold compared with *C*. For di-4-ANEPPS, the TBM artifact removal significantly decreased the power at the heart rate further (*C*: SM vs. TBM), making it equal to the power at 2 Hz above the heart rate (used as a proxy for the expected artifact free power at the heart rate). *C*: *statistically significant, ˣnon-significant differences between average power.

changes in fluorescence relative to the background fluorescence (i.e., ΔF/F) are measured on the same scale.

Spatial distribution of the BPA. To assess the spatial extent of the BPA as well as its correction, we compared the spatial distribution of the RMS of the BPA template with the spatial distribution of power at the heart rate of the raw as well as the BPA corrected data. Figure 5*A* indicates that the power at the heart rate is considerably reduced by the artifact removal. This was confirmed by statistical analysis of the shared variance (R^2) between the RMS of the BPA template and the power of the VSDI signal at the heart rate (Fig. 5*B* and Table 2). Overall, rmANOVA for di-4-ANEPPS revealed a significant effect of the artifact correction ($F = 16.348$, $P < 0.05$). The significant post hoc *t*-test contrast between the two BPA removal methods ($t = 3.850$, $P < 0.05$) indicates that the template-based artifact correction also showed from this point of view an additional improvement to the artifact correction, leaving only ~4.4% of shared variance over the imaged area between the RMS of the BPA and the power at the heart rate after removing the BPA with the TBM artifact correction.

Comparison of the (shot) noise levels of the two dyes. Figure 6*A* shows that the two dyes are practically identical in their noise level, as assessed by the RMS of baseline ΔF/F (i.e., shot noise) compared with the square root of the background fluorescence (Civillico and Contreras 2005). This is also reflected in the estimated coefficients of the second-order polynomial curve fit for the two dyes, as they do not differ significantly, i.e., all estimated coefficients for RH-1691 lie within the 95% confidence interval (CI) calculated for the di-4-ANEPPS coefficients: for the quadratic term $0.2419 \cdot 10^{-6}$–$0.3136 \cdot 10^{-6}$ (95 % CI = $0.2188 \cdot 10^{-6}$–$0.3140 \cdot 10^{-6}$), for the linear term $-0.6497 \cdot 10^{-4}$ to $-0.7604 \cdot 10^{-4}$ (95 % CI = $-0.7615 \cdot 10^{-4}$ to $-0.6048 \cdot 10^{-4}$) and for the constant 0.0054–0.0058, respectively (95 % CI = 0.0052–0.0058).

Similarly to Civillico and Contreras (2005), we compared the spatial distribution of the residuals of the curve fit. Since we were able to explicitly remove the BPA, we plotted the residuals after the BPA removal. As can be seen in Fig. 6*B*, for typical sections of the imaged area for both dyes, RH-1691 basically shows no systematic residuals (i.e., residuals that are related to vessels). di-4-ANEPPS on the other hand showed discrete residuals related to vessels but were far less pronounced than in the Civillico and Contreras (2005) paper (their Fig. 1, p. 174). Note that we used for reasons of comparability the same baseline and scaling as Civillico and Contreras (2005). Therefore, it can be concluded that the artifact correction considerably reduced systematic artifacts due to vessels and brain pulsation, especially for di-4-ANEPPS.

Correspondence of electrophysiology and imaging. For all conducted experiments, highly significant correlations between P1–N1 amplitude and the peak depolarization of the ROI, as measured by VSDI, were found (range: $r = -0.424$ to -0.7139, all $P < 0.01$). The correlation coefficients of RH-1691 and di-4-ANEPPS did not differ significantly ($t = 0.059$, $P > 0.5$; see Fig. 7*A*). Furthermore and interestingly, it can be seen that di-4-ANEPPS and RH-1691 do not at all scale differently but rather, show a high overall linear correlation of $r = -0.904$ ($P < 0.001$; Fig. 7*B*).

Spatial parameters of the optical response. The spatiotemporal development of the evoked VSDI response was assessed using data from all conducted experiments (i.e., from five di-4-ANEPPS experiments and aggregated over the seven RH-1691 experiments using two different electrophysiological recording setups). Figure 8, *A* and *B*, displays the spatiotemporal change in fractional fluorescence. Even when both dyes are scaled relative to their maximum change in fractional fluorescence, RH-1691 shows a more extended spatial spread as well as temporal prolongation of the response compared with di-4-ANEPPS. When the RH-1691 data are scaled equivalently to the di-4-ANEPPS experiments (see Fig. 8*B*), it can be seen that the change in fractional fluorescence is considerably stronger with RH-1691. Comparable with the several-fold larger P1–N1 amplitude found in the SEP recordings after application of RH-1691, the average maximum change in fractional fluorescence was found to be ~2.5-fold larger for RH-1691 (ΔF/F ~0.40%) than for di-4-ANEPPS (ΔF/F ~0.15%; Fig. 8*C*). Figure 8*E* provides the mean difference of the fractional fluorescence responses in the center of the image between the experiments conducted with di-4-ANEPPS and RH-1691. It can be seen that RH-1691 leads to a significantly higher and temporally more extended optical response from ~12 ms on up to 150 ms after deflection of the whisker. The spatially more extended response is evaluated in Fig. 8*C*. It

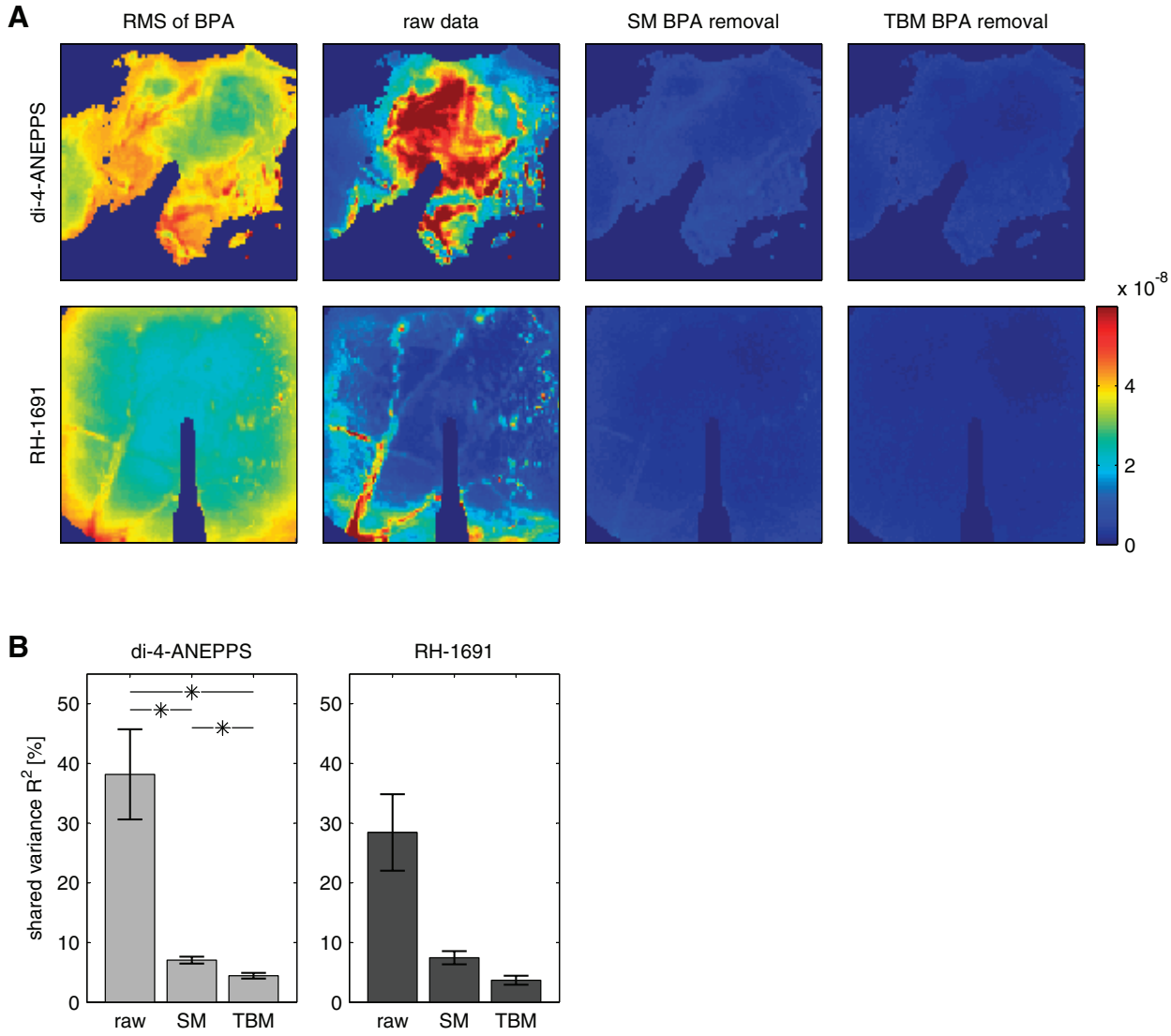

Fig. 5. Spatial distribution of the BPA. *A*: comparison of a representative di-4-ANEPPS and RH-1691 experiment; the *left-most image* in each row shows the distribution of the root mean square (RMS) of the BPA, i.e., the distribution of the BPA over the imaged area. The *images 2nd from left* illustrate the spatial distribution of the power at the heart rate in the raw data: for RH-1691, this appears to be more restricted to the vessels, whereas for di-4-ANEPPS, its distribution is less restrained to the vessels. The *3rd and 4th images* in each row show the distribution of power at the heartbeat frequency after the 2 artifact removal methods (same scaling as for raw data; see color bar). *B*: summary of the shared variance (R^2) between the RMS of the BPA (the distribution of the artifact) and the spatial power distribution at the heart rate for the raw data and after either artifact removal method, respectively (asterisks indicate significant contrasts; error bars indicate ±1 SE; note that statistical analysis was only conducted for di-4-ANEPPS).

may be noted that in principle, it is not possible to compare optical responses from different dyes directly. Nevertheless, since we have shown that the dyes have highly similar noise characteristics (Fig. 6*A*) and scale very similar with respect to electrophysiological responses (Fig. 7), it can be assumed that they scale very similar in their fluorescence responses and thus can be compared on a common scale. Finally, also in terms of qualitative aspects of the responses, the hyperpolarization observed with di-4-ANEPPS was not observed with RH-1691 (Fig. 8*D*).

Table 2. *Shared variance between the RMS of the BPA template and the power of the VSDI signal at the heart rate of the raw data, as well as after artifact correction with the 2 different methods*

	di-4-ANEPPS	RH-1691
Raw data	38.18 ± 8.45	28.45 ± 9.06
SM	7.04 ± 0.64	7.45 ± 1.57
TBM	4.44 ± 0.54	3.69 ± 1.07

Values are shared variance in percent ±1 SE. RMS, root mean square; BPA, brain-pulsation artifact; VSDI, voltage-sensitive dye imaging; SM, subtraction method; TBM, template-based method.

To estimate the spatial development and extent of the evoked VSDI response, we assessed the relative number of pixels showing a signal above a predetermined threshold over time. To ensure that potential differences in the spatial extent of the evoked response between the two dyes are not dependent on specific thresholds used, comparisons of the dyes for three differently defined thresholds are reported. Following the above-presented argument that the dyes scale almost identically in terms of their fractional fluorescence, we first chose 20% of the mean maximum activation within the first 20 ms

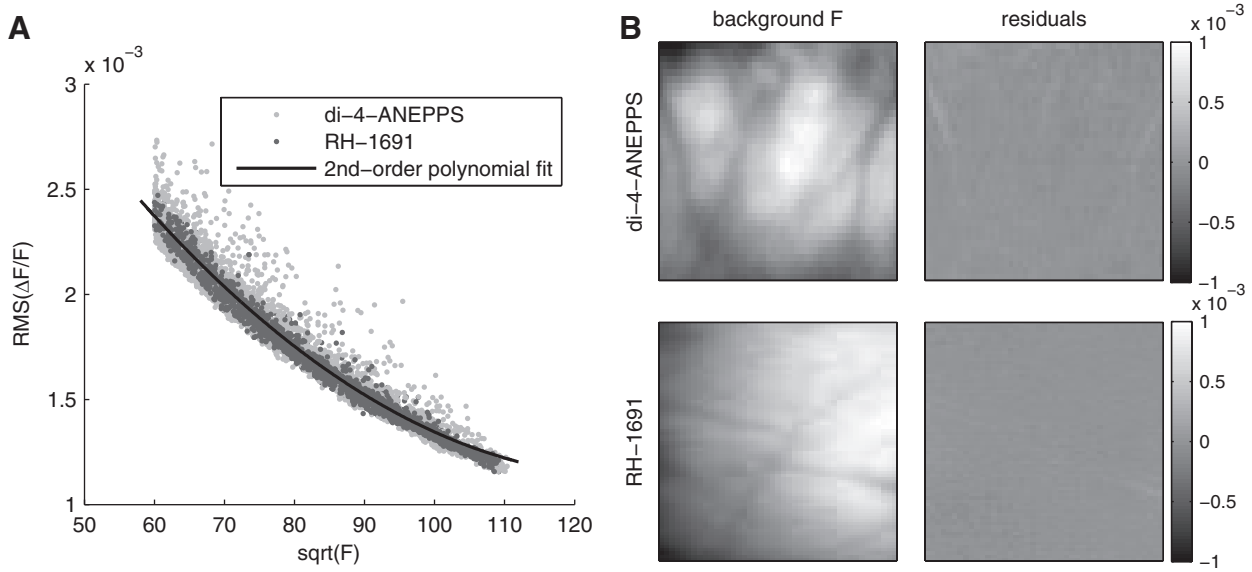

Fig. 6. *A*: relation of the square root (sqrt) of background fluorescence (F; i.e., brightness of stain) and RMS of baseline ΔF/F (i.e., shot noise) after TBM artifact removal; both dyes, plotted on top of each other, show the same scaling and level of shot noise, which was also confirmed statistically (see RESULTS). *B, left*: maps of background fluorescence showing sections of the imaged area that clearly contained vessels; *B, right*: residuals from 2nd-order polynomial fit for the same sections. For di-4-ANEPPS, discrete vessel-related residuals can be seen but are far less pronounced than reported previously [note that the same baseline and scaling were used as in Civillico and Contreras (2005)]. RH-1691 does not show any systematic residuals.

after stimulation over the five di-4-ANEPPS experiments (maximum activation = 0.15% ΔF/F) as a common and fixed threshold value. As shown in Fig. 9*A*, when using this common threshold, the maximum area of cortical activation amounted to 40.6% ± 6.9% (SE) of the imaged area for di-4-ANEPPS and was reached after 12–14 ms, whereas for RH-1691, almost the whole imaged area (87.1% ± 6.3%) was activated with a protraction of peak latency to 20–22 ms. For the RH-1691 experiments, it took ~150 ms compared with ~25 ms for di-4-ANEPPS for the evoked activity to return to the subthreshold baseline level. Figure 9 also provides the differences between the two dyes in the percentage of pixels showing suprathreshold fractional fluorescence together with the 95% CI of the difference. For the common threshold (Fig. 9*A*), significant differences between the dyes are observed between 10 ms and 76 ms. Figure 9*B* provides an attenuated but qualitatively similar picture when 20% of the mean maximum activation within the first 20 ms after stimulation within each experiment is used as a threshold (i.e., when explicitly controlling for the higher ΔF/F signal with RH-1691). Figure 9*C* shows that almost the same picture as with the common threshold emerged when using three times the RMS of the baseline fluorescence from −100 ms to stimulus onset as a threshold, which again reflects the fact that both dyes exhibit very similar noise characteristics. Taken together, it can be concluded that

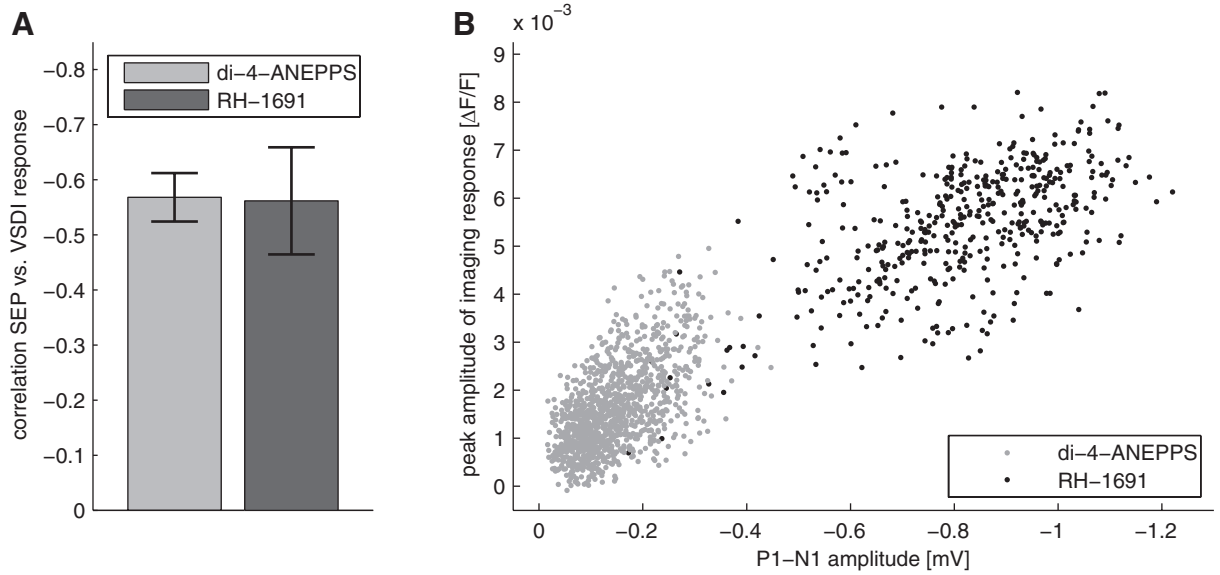

Fig. 7. *A*: average Pearson correlation coefficients of the 2 dyes for the correlation between the P1–N1 peak-to-peak amplitude and the peak amplitude of the voltage-sensitive dye imaging (VSDI) response in the ROI within 20 ms after whisker stimulation (error bars indicate ±1 SE). *B*: summary scatterplot of single-trial P1–N1 peak-to-peak amplitudes vs. the peak amplitude of the VSDI responses from all experiments conducted with the bipolar electrode.

RH-1691 leads to an increased spatial extent of the evoked response.

DISCUSSION

The current study had three major goals. First, we were to assess and re-assess potential pharmacological side effects of using the dyes di-4-ANEPPS and RH-1691 in an in vivo rodent somatosensory cortex preparation. Secondly, we were to evaluate a BPA removal algorithm proposed by Wu and colleagues (Lippert et al. 2007; Ma et al. 2004) and extend their approach to short trials of 2.4 s containing evoked activity, as well as compare its applicability to di-4-ANEPPS, which was not reported in detail previously. Finally, we were to compare the shot noise and BPA levels of both dyes and evaluate the implications regarding the SNR of both dyes.

Evaluation of pharmacological side effects. The data from this study provide evidence that application of RH-1691 has strong pharmacological side effects and considerably changes the responsiveness of cortical tissue to sensory stimulation. This interpretation is based on the following observations. *1*) SEP responses, as measured by the P1–N1 peak-to-peak amplitude, reliably increased several-fold after application of RH-1691 compared with the stable pre-dyeing baseline recordings (Fig. 1). We have shown that this observation is not attributable to changes or differences in the anesthetic levels and that the same picture emerged when restricting the analysis to trials having been recorded at a moderate level of anesthesia. *2*) Not only did the SEP responses increase but, importantly, components of the SEP also significantly changed shape (e.g., the combination of increased amplitude and latency shift of the N1 in Fig. 1*A*), suggesting a considerable change of the network dynamics of the somatosensory system in response to external stimulation after application of RH-1691. Both observations are in compelling contrast to the di-4-ANEPPS data showing only a transient increase of SEP response during dyeing, which resolved completely by the time imaging commenced (Fig. 1*A*); this was confirmed statistically by a near-perfect 0-lag cross-correlation between the signals before dyeing with di-4-ANEPPS and during imaging, in addition to a lack of statistical difference between the P1–N1 amplitude during the pre-dyeing baseline compared with the imaging period. *3*) Both dyes scaled equivalently in terms of the RMS of ΔF/F in the prestimulus period before sensory stimulation (Fig. 6*A*), i.e., showed exactly the same shot noise characteristics. This observation was also corroborated by the finding that both dyes showed equivalent power values in the FFT spectra at different frequencies (Fig. 4*C*). Furthermore, a strong overall linear correlation between SEP amplitudes and amplitudes of the VSDI responses was observed (Fig. 7), which indicates that the dyes also scaled equivalently with respect to their relationship between changes of ΔF/F per unit change of the electrophysiological signal. Thus the stronger VSDI signal found with RH-1691 directly reflected the changes in the electrophysiological recordings. *4*) The change in dynamics of the evoked response was corroborated further by the spatiotemporal expansion of the evoked VSDI response (Figs. 8 and 9*A*): whereas for di-4-ANEPPS, an activation of ~40% of the imaged area was observed after sensory stimulation and lasted for ~25 ms, after staining with RH-1691, ~90% of the imaged area was activated above threshold after stimulation, reaching the maximal area of activation later and lasting up to 150 ms. It should be noted that the spatiotemporal activation pattern of the evoked ΔF/F responses reported for RH-1691 (Fig. 8, *B* and *D*) is comparable with other published data [e.g., Ferezou et al. 2006 (their Fig. 3, *B* and *E*); Lippert et al. 2007 (their Fig. 5); Petersen et al. 2003 (their Fig. 1*I*)] and does not seem to be unique to the specific experimental setup and methods that we used in our study. Furthermore, we also argue that attribution of the pronounced increase in SEP amplitude for RH-1691 to photodynamic or phototoxic effects caused by strong illumination is unlikely for two reasons. *1*) SEP amplitude was already strongly increased during staining when no illumination of the tissue took place; in fact, the imaging room was kept completely dark as soon as the dye was applied, and only weak, indirect light was used when necessary for manipulations, e.g., changing of dye solution, etc. *2*) Similarly to Lippert and colleagues (2007), we recorded very stable SEP signals over 2–3 h of imaging (see Fig. 1, *B* and *C*) [Lippert et al. 2007 (their Fig. 6)]. Thus we believe that illumination of the tissue and photodynamic or phototoxic effects can be ruled out as a major factor for the increased evoked responses. Taken together, it is concluded that the application of RH-1691 significantly changed the amplitude as well as the dynamics of the neural response to sensory stimulation.

Nevertheless, it should also be noted that in contrast to the effects on evoked responses, application of neither dye had a detectable influence on the spontaneous, ongoing activity as measured by the spectral content of the EEG (Fig. 2). First, no significant changes of the relative frequencies of three different surgical anesthetic states before and after application of the dyes were found (Table 1), indicating that the dyes had no systemic effect in the sense of changing the level of cortical arousal. Secondly, statistical comparison of the spectral content of the EEG before and after application of the dyes did not reveal any systematic statistical differences in the spectral content of the EEG up to 100 Hz between the baseline and imaging periods. Taken together, this points to a dissociation of the pharmacological effects of RH-1691, with a strong effect on sensory-evoked activity but no detectable effect on the ongoing EEG.

To the best of our knowledge, there are no in vivo studies published that report a systematic assessment of baseline electrophysiological recordings before dyeing with subsequent continuation of electrophysiological recordings during dyeing and imaging. For example, in the study of Tsodyks and colleagues (1999), electrodes were placed after dyeing [as described in Arieli et al. (1995); see also Petersen et al. (2003)], which seems to be true for the majority of in vivo studies. Importantly, in the papers by Shoham and colleagues (1999) and Slovin and colleagues (2002), introducing the new blue dyes RH-1692 and RH-1691, we could not find electrophysiological data that would allow direct comparison of the pharmacological side effect as observed and reported in the current study (i.e., comparison of a baseline recording with subsequent equivalent recordings during imaging). Nevertheless, potential pharmacological side effects clearly were assessed and discussed in both papers in terms of intrinsic optical imaging (revealing ocular-dominance columns) and with respect to monitoring the deterioration of neural signals during imaging. Generally, there seems to be a bias toward the expectation and concern that any dye would rather decrease

and deteriorate neural activity [Shoham et al. 1999 (their section *Other effects of the dye*, p. 797); see also Lippert et al. 2007], and as a consequence, increased responses in in vivo experiments may actually have been overlooked so far. In this context, it is important to note that within our study, the topographical confinement of the initial evoked response (up to ~10 ms) to the C2 barrel of the posterior–medial barrel subfield was not affected. That is, the early part of the evoked optical response clearly originates from and is confined to one barrel (~500 μm); only later parts of the optical response show distinctly different spatiotemporal characteristics. Thus the current study does not necessarily invalidate or question the

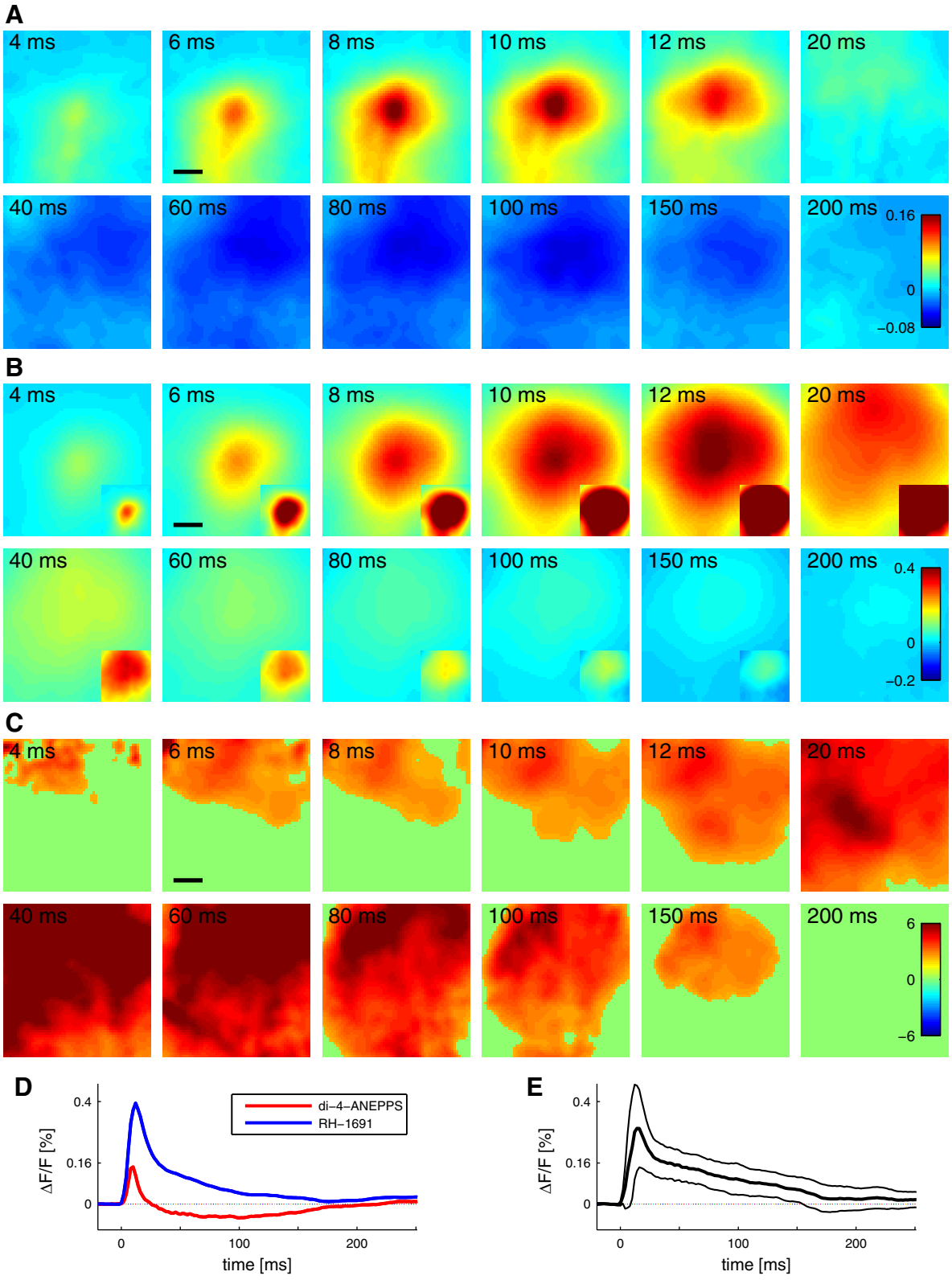

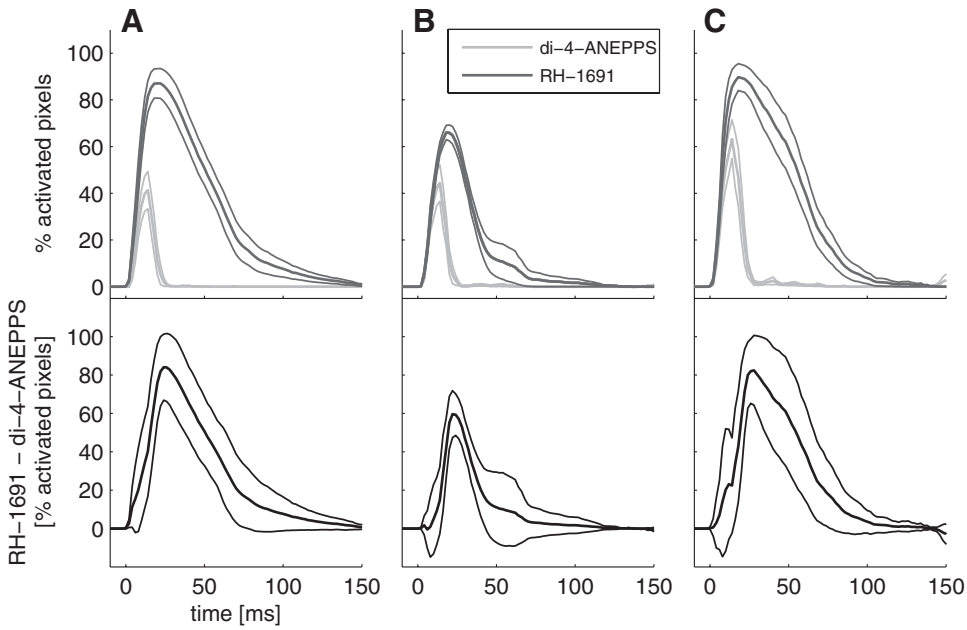

Fig. 9. Extent of the spatial activation over time expressed as percentage of "activated" pixels above 3 differently defined thresholds (*top plots*); light lines indicate ±1 SE. *Bottom plots* show the mean difference between di-4-ANEPPS ($n = 5$) and RH-1691 ($n = 7$) experiments; light lines indicate the 95% CI for the mean difference. *A*: percentage of pixels showing fractional fluorescence above a common fixed threshold (20% of the mean maximum activation within the 1st 20 ms after stimulation over the 5 di-4-ANEPPS experiments). For RH-1691, ~90% of the whole imaged area shows suprathreshold-evoked activation, and the temporal dynamics of the activation is clearly different from the di-4-ANEPPS experiments. *B*: threshold defined as mean maximum activation within the 1st 20 ms after stimulation within each experiment. *C*: threshold defined as 3 times the RMS of the baseline fluorescence from −100 ms to stimulus onset.

earlier evaluations of RH-1691 cited above; rather, it adds another perspective on spatiotemporal dynamics and characteristics of evoked responses in vivo which, so far, have not been the focus of evaluations of pharmacological side effects when using fluorescent dyes such as di-4-ANEPPS and RH-1691 in vivo.

With regard to the potential causes and mechanisms underlying the suggested pharmacological side effect, we can only speculate in the context of the data provided in this report. A recent study by Mennerick and colleagues (2010) found potentiation of $GABA_A$ receptor currents in the presence of a number of VSDs including di-4-ANEPPS and RH-1691. Some observations made by Mennerick and colleagues (2010) parallel our findings and may be noteworthy. First, even though both dyes have been found to positively modulate $GABA_A$ receptors, dynamics for $GABA_A$ receptor currents under di-4-ANEPPS were qualitatively different from receptor currents under RH-1691. Coapplication of GABA with di-4-ANEPPS slowly increased receptor currents over 30 s, whereas coapplication of GABA with RH-1691 led to an initial peak in $GABA_A$ receptor currents followed by a marked decrease [Mennerick et al. 2010 (their Figs. 1*B* and 2*A*)]. This implies that at the receptor level, the kinetics of the receptor-dye interaction are different for both dyes. Second, prolonged incubation of hippocampal cultures with di-4-ANEPPS led first to a pronounced decrease in spiking network activity with a strong rebound in activity over the course of 2 h, reaching baseline levels after washout of unbound dye. This also parallels our observation of transient changes of SEPs during dyeing but otherwise, unaltered SEPs after washing out of di-4-ANEPPS when imaging commenced. It may be possible that di-4-ANEPPS exerts its effects on $GABA_A$ receptors mainly when unbound in the medium, allowing a return to baseline activity once the unbound fraction of the dye gets internalized into the cell membrane or the cell or is washed out. Unfortunately, Mennerick and colleagues (2010) provided only data for long incubation with di-4-ANEPPS but not for RH-1691; it would be interesting to see whether RH-1691 would exhibit long-lasting effects on the excitability of cortical tissue as reported here. Additionally, RH-1691 showed a dye concentration-dependent "biphasic" effect on $GABA_A$ receptor functioning with lower potentiation of $GABA_A$ receptor currents for higher concentrations of the dye. Taken together, the different behavior of the two dyes investigated in the current study is not completely unexpected.

However, the increase in excitability due to application of the dyes in the current study cannot be explained directly by the findings of Mennerick and colleagues (2010). In general, it is not easy to extrapolate neural dynamics at the systems level from findings at the level of small networks in vitro or at the level of receptors, and it should also be noted that dye concentrations, labeling solutions, incubation times, neural tissue under investigation, as well as other parameters differed greatly in the study by Mennerick and colleagues (2010) compared with the current study. It also cannot be excluded at the current stage that the dyes, given their amphiphilic nature, also interact with other receptors and channels on membranes of the neural tissue. In this context, it may be noteworthy that

Fig. 8. Mean VSDI activation patterns evoked by a single deflection of *whisker C2* for di-4-ANEPPS (*A*; $n = 5$) and RH-1691 (*B*; imaging data aggregated over the 2 electrophysiology setups; $n = 7$). Time after stimulus onset is displayed in the *top-left corners*; note the change in time intervals at the end of the *1st* and in the *2nd row*. The color bars illustrate the scaling in ΔF/F; note that the scaling for RH-1691 is 2.5-fold compared with the scaling for di-4-ANEPPS. Insets in *B* show the same data with the scaling of di-4-ANEPPS. Even when scaled relative to the maximal change in ΔF/F, RH-1691 shows a different spatial expansion compared with di-4-ANEPPS and no hyperpolarization. *C*: estimation of the difference between the di-4-ANEPPS and RH-1691 experiments. Indicated are significant *t*-values (at the $P < 0.05$ level) from 2-sample *t*-tests/frame and pixel. Note that this analysis was conducted to provide an overview of the highly systematic difference in the spatiotemporal activation pattern of the 2 dyes; thus the *t*-values should be interpreted as effect size measures and not in the sense of inferential statistical parameters. *D*: time course of the average change in fractional fluorescence for the 2 dyes at the center of the image (corresponding to *barrel C2*). *E*: difference between the average changes in fractional fluorescence for the 2 dyes at the center of the image (bold line) with the 95% confidence interval (CI) of the difference (surrounding light lines). Scale bars in *A–C*: 500 μm.

the dissociation of effects on different cortical pathways has also been observed with topical application of cholinergic agents (Oldford and Castro-Alamancos 2003), which have also been shown to enhance the functional representation of sensory inputs (Penschuck et al. 2002). Further research will be required to elucidate the exact locus of action of the dyes at the systemic level.

Evaluation of artifact removal. The dominating physiological noise in in vivo VSDI recordings is the pulsation of the vessels and brain tissue caused by the pulse wave from the heartbeat. Any in vivo preparation needs to overcome this specific artifact. Two major routes of removing this BPA have been proposed previously in the literature: the subtraction of subsequently recorded trials time locked to the ECG (SM) and a template-based algorithm making use of the fact that the BPA is very stereotypical and time locked to the R-wave of the ECG (TBM). Since the TBM BPA removal was evaluated previously in detail by Lippert and colleagues (2007) for RH-1691, we focused the evaluation on di-4-ANEPPS and compared the two artifact removal methods with a focus on the red dye.

Figure 3 provides an overview of the effects of the two different artifact removal techniques for a ROI taken from a single VSDI recording after staining with di-4-ANEPPS. As described, evaluation of the performance of either artifact removal method by means of FFT spectra revealed a clear reduction of the heart rate-associated peaks in the FFT spectrum for both artifact removal methods, which was statistically confirmed. However, importantly, it was shown that the SM is susceptible to subtle shifts in the heartbeat frequency and spontaneous activity in the subsequent trial, leading to the introduction of artificial "activity". Consequentially, the TBM significantly decreased the heartbeat frequency-associated power farther down to the expected artifact-free power level, and no residual peaks were found in the spectrum after TBM artifact correction. The effect of spontaneous activity within the subsequent no-stimulus trial was demonstrated in Fig. 3*A*: between 0.3 and 0.5 s, a marked negative shift in the VSDI signal was observed, which could be attributed to spontaneous activity in the subsequent trial (Fig. 3*B*). This was found to be reflected in changes in the FFT spectrum at frequencies not associated with the heartbeat frequency (Fig. 3*C*).

The summary of all di-4-ANEPPS experiments (Fig. 4) confirmed the picture found for the single trial. Both artifact removal methods significantly reduced the BPA-associated power, but whereas the SM artifact correction showed some residual power at the heart rate, the TBM reduced the power significantly farther to the expected artifact-free power level.

Comparing the spatial distribution of the BPA (Fig. 5) before and after artifact removal also supports the finding that the TBM artifact removal worked well in removing the BPA. Initially, a large amount of R^2 between the spatial distribution of power at the heartbeat frequency and the RMS of the BPA was observed. Both artifact correction methods showed the same picture as for the FFT analyses: SM and TBM significantly reduced R^2, thus showing a dissociation of the spatial distribution of power at the heart rate and the BPA, but also here, TBM significantly decreased R^2 further. Thus we conclude that the TBM BPA removal works well for short trials of 2.4 s recorded with di-4-ANEPPS as the VSD, which to our knowledge, has not been shown previously.

Comparison of noise characteristics of di-4-ANEPPS and RH-1691. The raw BPA-associated power was ~4.5-fold stronger for di-4-ANEPPS than for RH-1691 (Fig. 4*B*). This confirms that the BPA is indeed stronger for red dyes as reported previously (Civillico and Contreras 2005). After optimal BPA removal with the TBM, however, both dyes exhibited exactly the same power level, thus indicating that the general signal level and signal strength do not differ for both dyes when the BPA is removed successfully.

The comparison of the shot noise levels for the two dyes supports this finding. In contrast to Civillico and Contreras (2005), we imaged both dyes at the same absolute levels of fluorescence, thus making the shot noise characteristics (as estimated by the RMS of the baseline ΔF/F) of the two dyes directly comparable. As mentioned already above, the two dyes showed exactly the same relation between square root background fluorescence and the RMS of baseline ΔF/F (Fig. 6*A*), which was also confirmed statistically. Therefore, it can be concluded that the general shot noise levels of the two dyes did not differ.

Comparison of SEP and VSDI responses and implications for SNR. Figure 7*A* shows that the linear correlations between the P1–N1 amplitude and the amplitude of the VSDI response are almost identical for both dyes; statistically, the correlation coefficients of RH-1691 and di-4-ANEPPS did not differ. More interestingly, Fig. 7*B* suggests that the two dyes do not at all scale differently in terms of ΔF/F. Rather, an overall linear relationship between the SEPs and the VSDI responses was established. In terms of the SNR, the important implication of this observation is that the increased VSDI response observed with RH-1691, showing a clear linear relationship to the SEPs, is rather a consequence of the changed physiology of the preparation, as expressed in the distinctly changed SEPs compared with the pre-dye baseline recordings. Thus the gain in SNR cannot be attributed to superior properties of RH-1691 in terms of reduced noise levels (see above) or a steeper dynamic range and correlation between electric potential and fractional fluorescence changes but is a consequence of the artificially increased signal due to the increased responsiveness of the cortical tissue.

Conclusions. We have provided evidence that RH-1691 in the rodent somatosensory preparation under investigation leads to strong pharmacological side effects as reflected in the artificially increased responsiveness of the neural tissue to sensory stimulation. Thus the superior SNR implicated for RH-1691 from this point of view is not a consequence of reduced noise or a changed dynamic range of the dye but, rather, a consequence of the artificially increased signal. In fact, both dyes have shown equivalent shot noise characteristics and, given the equivalent scaling of the two dyes, it must be concluded that the SNR is similar for both dyes. It has also been shown that there is a dissociation of pharmacological side effects: whereas sensory-evoked responses were increased, the spectral content of the ongoing EEG was not changed systematically by application of RH-1691, indicating that the spontaneous background activity is not measurably affected by RH-1691.

The use of di-4-ANEPPS in in vivo preparations has not been reported previously, aside from our own work (Devonshire et al. 2010a, b) yet, as we show here, provides stable imaging recordings up to 4 h with no apparent change in the

basic physiology of the preparation. Furthermore, evaluation of a BPA removal algorithm by Wu and colleagues (Lippert et al. 2007; Ma et al. 2004) has proven to be very powerful in specifically removing the BPA from images acquired following di-4-ANEPPS staining. Thus if RH-1691 is only preferred due to the absence (or reduction) of the BPA (Civillico and Contreras 2005), then the template-based BPA removal algorithm largely solves this particular problem and allows use of dyes that show a priori stronger BPA but do not change the physiology of the system under investigation. Thus we share the preference of Civillico and Contreras (2005) for a red dye and have shown that its applicability is strongly improved by applying the TBM BPA removal algorithm, making it a valuable tool for neurophysiological and neuropharmacological research where changes in basic neural activity are not desirable.

ACKNOWLEDGMENTS

We thank the three anonymous reviewers of the manuscript for their help and guidance.

Present address of T. H. Grandy: Max Planck Institute for Human Development, Center for Lifespan Psychology, Lentzeallee 94, 14195 Berlin, Germany.

GRANTS

Support for this work was funded by grants from the Mind Science Foundation and the James Martin 21st Century School.

DISCLOSURES

No conflicts of interest, financial or otherwise, are declared by the authors.

AUTHOR CONTRIBUTIONS

Author contributions: T.H.G., S.A.G., and I.M.D. conception and design of research; I.M.D. performed experiments; T.H.G. and I.M.D. analyzed data; T.H.G., S.A.G., and I.M.D. interpreted results of experiments; T.H.G. prepared figures; T.H.G., S.A.G., and I.M.D. drafted manuscript; T.H.G., S.A.G., and I.M.D. edited and revised manuscript; T.H.G., S.A.G., and I.M.D. approved final version of manuscript.

REFERENCES

Angel A. The G. L. Brown lecture. Adventures in anaesthesia. *Exp Physiol* 76: 1–38, 1991.

Arieli A, Shoham D, Hildesheim R, Grinvald A. Coherent spatiotemporal patterns of ongoing activity revealed by real-time optical imaging coupled with single-unit recording in the cat visual cortex. *J Neurophysiol* 73: 2072–2093, 1995.

Borgdorff AJ, Poulet JF, Petersen CC. Facilitating sensory responses in developing mouse somatosensory barrel cortex. *J Neurophysiol* 97: 2992–3003, 2007.

Civillico EF, Contreras D. Comparison of responses to electrical stimulation and whisker deflection using two different voltage-sensitive dyes in mouse barrel cortex in vivo. *J Membr Biol* 208: 171–182, 2005.

Collins TF, Mann EO, Hill MR, Dommett EJ, Greenfield SA. Dynamics of neuronal assemblies are modulated by anaesthetics but not analgesics. *Eur J Anaesthesiol* 24: 609–614, 2007.

Devonshire IM, Dommett EJ, Grandy TH, Halliday AC, Greenfield SA. Environmental enrichment differentially modifies specific components of sensory-evoked activity in rat barrel cortex as revealed by simultaneous electrophysiological recordings and optical imaging in vivo. *Neuroscience* 170: 662–669, 2010a.

Devonshire IM, Grandy TH, Dommett EJ, Greenfield SA. Effects of urethane anaesthesia on sensory processing in the rat barrel cortex revealed by combined optical imaging and electrophysiology. *Eur J Neurosci* 32: 786–797, 2010b.

Devonshire IM, Preston MJ, Dommett EJ, Murphy KL, Greenfield SA. Design and evaluation of a low-cost respiratory monitoring device for use with anaesthetized animals. *Lab Anim* 43: 382–389, 2009.

Di S, Barth DS. Topographic analysis of field potentials in rat vibrissa/barrel cortex. *Brain Res* 546: 106–112, 1991.

Ferezou I, Bolea S, Petersen CC. Visualizing the cortical representation of whisker touch: voltage-sensitive dye imaging in freely moving mice. *Neuron* 50: 617–629, 2006.

Ferezou I, Haiss F, Gentet LJ, Aronoff R, Weber B, Petersen CC. Spatiotemporal dynamics of cortical sensorimotor integration in behaving mice. *Neuron* 56: 907–923, 2007.

Friedberg MH, Lee SM, Ebner FF. Modulation of receptive field properties of thalamic somatosensory neurons by the depth of anesthesia. *J Neurophysiol* 81: 2243–2252, 1999.

Grinvald A, Anglister L, Freeman JA, Hildesheim R, Manker A. Real-time optical imaging of naturally evoked electrical activity in intact frog brain. *Nature* 308: 848–850, 1984.

Grinvald A, Hildesheim R. VSDI: a new era in functional imaging of cortical dynamics. *Nat Rev Neurosci* 5: 874–885, 2004.

Lippert MT, Takagaki K, Xu W, Huang X, Wu JY. Methods for voltage-sensitive dye imaging of rat cortical activity with high signal-to-noise ratio. *J Neurophysiol* 98: 502–512, 2007.

Loew LM. Potentiometric dyes: imaging electrical activity of cell membranes. *Pure Appl Chem* 68: 1405–1409, 1996.

Loew LM, Cohen LB, Dix J, Fluhler EN, Montana V, Salama G, Wu JY. A naphthyl analog of the aminostyryl pyridinium class of potentiometric membrane dyes shows consistent sensitivity in a variety of tissue, cell, and model membrane preparations. *J Membr Biol* 130: 1–10, 1992.

Ma HT, Wu CH, Wu JY. Initiation of spontaneous epileptiform events in the rat neocortex in vivo. *J Neurophysiol* 91: 934–945, 2004.

Mann EO, Suckling JM, Hajos N, Greenfield SA, Paulsen O. Perisomatic feedback inhibition underlies cholinergically induced fast network oscillations in the rat hippocampus in vitro. *Neuron* 45: 105–117, 2005.

Mennerick S, Chisari M, Shu HJ, Taylor A, Vasek M, Eisenman LN, Zorumski CF. Diverse voltage-sensitive dyes modulate GABAA receptor function. *J Neurosci* 30: 2871–2879, 2010.

Oldford E, Castro-Alamancos MA. Input-specific effects of acetylcholine on sensory and intracortical evoked responses in the "barrel cortex" in vivo. *Neuroscience* 117: 769–778, 2003.

Penschuck S, Chen-Bee CH, Prakash N, Frostig RD. In vivo modulation of a cortical functional sensory representation shortly after topical cholinergic agent application. *J Comp Neurol* 452: 38–50, 2002.

Petersen CC, Grinvald A, Sakmann B. Spatiotemporal dynamics of sensory responses in layer 2/3 of rat barrel cortex measured in vivo by voltage-sensitive dye imaging combined with whole-cell voltage recordings and neuron reconstructions. *J Neurosci* 23: 1298–1309, 2003.

Schaffer P, Ahammer H, Muller W, Koidl B, Windisch H. Di-4-ANEPPS causes photodynamic damage to isolated cardiomyocytes. *Pflugers Arch* 426: 548–551, 1994.

Shoham D, Glaser DE, Arieli A, Kenet T, Wijnbergen C, Toledo Y, Hildesheim R, Grinvald A. Imaging cortical dynamics at high spatial and temporal resolution with novel blue voltage-sensitive dyes. *Neuron* 24: 791–802, 1999.

Slovin H, Arieli A, Hildesheim R, Grinvald A. Long-term voltage-sensitive dye imaging reveals cortical dynamics in behaving monkeys. *J Neurophysiol* 88: 3421–3438, 2002.

Tominaga T, Tominaga Y, Yamada H, Matsumoto G, Ichikawa M. Quantification of optical signals with electrophysiological signals in neural activities of Di-4-ANEPPS stained rat hippocampal slices. *J Neurosci Methods* 102: 11–23, 2000.

Tsodyks M, Kenet T, Grinvald A, Arieli A. Linking spontaneous activity of single cortical neurons and the underlying functional architecture. *Science* 286: 1943–1946, 1999.

Waggoner AS, Grinvald A. Mechanisms of rapid optical changes of potential sensitive dyes. *Ann N Y Acad Sci* 303: 217–241, 1977.